Nonlinear Analysis of Reinforced Concrete Roof Using Shell Elements

Analyse non-linéaire de toitures en béton armé, à l'aide d'éléments de coques

Nichtlinearer Berechnung eines Betondachtragwerks mit Hilfe von Schalenelementen

Ole STRØM
Doctor Engineer
Veritas Research
Høvik, Norway

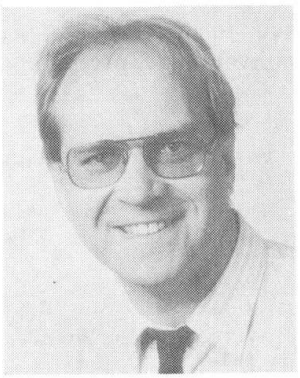

Ole Strøm, born 1958, got his civil and doctor's engineering degree at the Norwegian Institute of Technology, Trondheim, Norway. For the last four years he has worked with the nonlinear finite element program FENRIS, and then mainly with reinforced concrete.

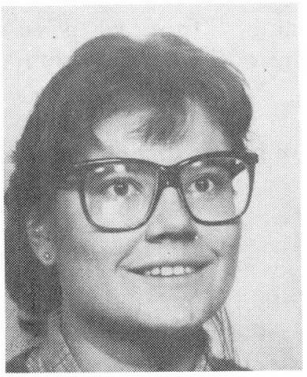

Anne Vasbotten, born 1962, got her civil-engineering degree at the Norwegian Institute of Technology, Trondheim, Norway. Her diploma work was about reinforced concrete roofs using shell elements.

Anne VASBOTTEN
Civil Engineer
Norwegian Inst. of Techn.
Trondheim, Norway

SUMMARY

This paper deals with nonlinear finite element analyses of reinforced concrete shell roofs. Four noded shell elements, based on the theory of free formulation, are used together with a nonlinear concrete- and reinforcement-model. The general elastic-plastic flow theory is combined with the load surface theory of Chen and Chen. This theory allows for different properties in tension and compression. Hardening, cracking and crushing are handled. Smeared cracking with two independent crack directions may be introduced when cracking.

RÉSUMÉ

L'article a pour objet l'analyse de coques en béton armé par la méthode des éléments finis non-linéaires. Des éléments de coques à quatre noeuds basés sur la théorie de la formulation libre sont utilisés en même temps qu'un modèle non-linéaire de béton et de renforcement. La théorie générale d'écoulement élastique-plastique est combinée avec la théorie des charges superficielles de Chen et Chen. Cette dernière théorie permet de considérer des propriétés différentes en tension et en compression. Le durcissement, la fissuration et l'écrasement sont étudiés. Des fissurations homogénéisées avec deux directions indépendantes peuvent être introduites.

ZUSAMMENFASSUNG

In diesem Beitrag werden nicht-lineare Finite-Elemente-Analysen für Schalendecken aus Stahlbeton durchgeführt. Dabei werden vier Knotenelemente unter Zugrundelegung der Theorie der freien Formulierung zusammen mit einem nicht-linearen Modell für Beton und Stahl angewandt. Die allgemeine elasto-plastische Fliesstheorie wird mit der Grenzflächentheorie von Chen u. Chen kombiniert. Die Theorie erlaubt die Anwendung verschiedener Eigenschaften für Zug- und Druckbelastung. Erhärtung, Rissbildung und Druckversagen werden behandelt. Die Bildung von ausgeglichenen Rissen mit zwei unabhängigen Rissrichtungen kann auch eingeführt werden.

1. THE QUADRILATERAL SHELL ELEMENT

The four noded shell element is based on the free formulation [1,2]. This element is initially planar and has three translational and three rotational freedoms per corner node. The convergence of the elements, which is well documented in [1,2], are assured through satisfaction of the so-called "individual element test".

The incremental equilibrium is expressed through the relation

$$\Delta \mathbf{S}_{int} = \mathbf{k}_T \Delta \mathbf{v} = (\mathbf{k}_{mat} + \mathbf{k}_{geom})\Delta \mathbf{v} \tag{1}$$

The tangential or incremental stiffness $\mathbf{k}_T$ is comprised of material and geometric stiffness contributions. The material stiffness is obtained from the convential expression

$$\mathbf{k}_{mat} = \int_V \mathbf{B}^T \mathbf{C}_T \mathbf{B} dV \tag{2}$$

where $\mathbf{C}_T$ is the tangential or incremental material law. The strain-producing matrix, $\mathbf{B}$, is given by

$$\mathbf{B} = \frac{1}{V}\mathbf{L}^T + \tilde{\mathbf{B}}_{qh}\mathbf{H}_h \tag{3}$$

Where V is the volum of the element, and $\mathbf{L}$ is the so-called "lumping matrix". $\tilde{\mathbf{B}}_{qh}$ is "energy orthogonal" with respect to the rc-modes. $\mathbf{H}_h$ is the inverted, generalized h-modes [1,2].

The geometric stiffness matrix $\mathbf{k}_{geom}$ for a flat shell element may be derived from the incremental form of the virtual work principle. The geometric stiffness for in-plane (membrane) action is uncoupled with the out-of-plane (bending) action [1,2].

In the co-rotated reference system the internal, element nodal reaction forces $\mathbf{S}_{int.}$ is found from the usual expression

$$\mathbf{S}_{int} = \int_V \mathbf{B}^T \sigma dV \tag{4}$$

Where σ is the Cauchy stress.

The forces and stiffness matrices are found by using two by two Gausian integration over the area of the quadrilaterial. Over the thickness eight Lobatto points are used.

2. THE COROTATED "GHOST" REFERENCE DESCRIPTION

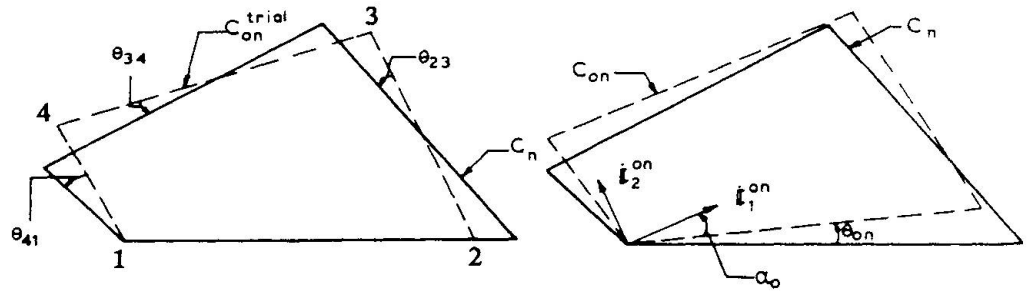

Fig. 1 Quadrilateral shell element in deformed and corotated configuration

A Langrian description of the displacements is used. The deformation of each element is referred to the initial configuration of each element. This reference configuration, C_{on}, is closely displaced and rotated along with the deformed configuration in order to minimize the rigid-body part of the rotational motion.

The direction of the local x-axis goes through nodes 1 and 2 of the "ghost" reference C_{on}. The normal to the plane of the "ghost" reference is taken as the vector formed by the cross-product of the vectors formed by the two diagonals of the deformed element. The corners 2, 3 and 4 of the warped quadrilateral are projected onto the reference plane. The "ghost" reference C_{on} is then rotated in its plane such that the sum of the squared deviatoric angles Θ_{ij} from the projected element C_n is minimized [1,2], see Fig. 1. The "ghost" reference will then be objective with respect to the rotations.

3. THE FLOW THEORY BY CHEN AND CHEN

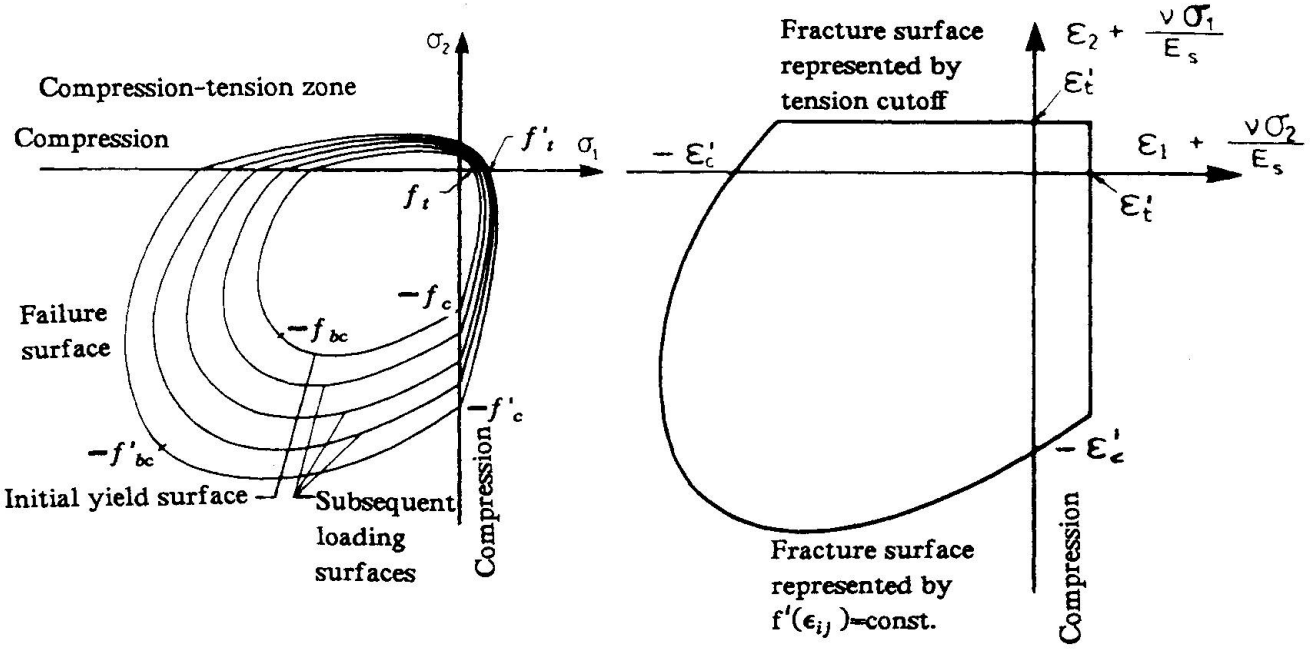

Fig. 2 a) Loading surfaces of concrete in the biaxial stress plane. b) Fracture surface defined by strain components in the biaxial strain plane.

Chen and Chen postulated an initial, non-smooth yield surface with subsequent loading surfaces, and a failure surface for concrete. These surfaces in two-dimensional principal stress space are traced in Fig. 2a. The concrete is treated as an elastic-plastic strain hardening material with fracturing behaviour in tension.

Three mathematical equations are used to define Chen and Chen's loading surfaces [3,4,5] :

1) An initial discontinuous loading surface

$$f_o = \sqrt{J_2^\sigma - \frac{1}{12}(I_1^\sigma)^2 \pm \frac{1}{12}(I_1^\sigma)^2 + \frac{A_o}{3}I_1^\sigma} - \tau_o \tag{5}$$

2) Subsequent loading surfaces

$$f = \frac{\sqrt{J_2^\sigma - \frac{1}{12}(I_1^\sigma)^2 \pm \frac{1}{12}(I_1^\sigma)^2 + \frac{\beta}{3}I_1^\sigma}}{\sqrt{1 - \frac{\alpha}{3}I_1^\sigma}} - \tau \tag{6}$$

3) An ultimate failure loading surface

$$f_u = \sqrt{J_2^\sigma - \frac{1}{12}(I_1^\sigma)^2 \pm \frac{1}{12}(I_1^\sigma)^2 + \frac{A_u}{3}I_1^\sigma} - \tau_u \tag{7}$$

The material constants, A_o, τ_o, A_u and τ_u are functions of the material parameters f_c, f'_c, f_t, f'_t, f_{bc} and f'_{bc}, see Fig. 2a. Here, f'_c, f'_t and f'_{bc} denote the ultimate strength of concrete under uniaxial compressive loading, uniaxial tensile loading, and equal biaxial compressive loading, respectively, while f_c, f_t and f_{bc} denote the initial yield strength of concrete under uniaxial compressive loading, uniaxial tensile loading and equal biaxial compressive loading. The positive-negative sign in the third term in Eqs. (5) to (7) represents the loading function in the "compression-compression zone" and the "tension-compression and tension-tension zone", respectively. The loading surfaces, which are functions of the history of loading, are derived from an isotropic expansion of the initial yield surface, until coincidence with the failure surface f_u is reached. The failure surface f_u is the outmost extreme loading surface. The constants α and β are found by the claim that the loading surface shall coincide with the initial yield surface and the failure surface as extreme cases.

For the case of plane stress ($\sigma_{zz} = \sigma_{xz} = \sigma_{yz} = 0$) the incremental stress strain relation will be [3] :

$$\begin{Bmatrix} d\sigma_{xx} \\ d\sigma_{yy} \\ d\sigma_{xy} \end{Bmatrix} = \frac{E_o}{(1-\nu^2)} \begin{bmatrix} 1-\omega\Phi_{11} & \nu-\omega\Phi_{12} & -\omega\Phi_{13} \\ & 1-\omega\Phi_{22} & -\omega\Phi_{23} \\ & & \frac{(1-\nu)}{2}-\Phi_{33} \end{bmatrix} \begin{Bmatrix} d\varepsilon_{xx} \\ d\varepsilon_{yy} \\ 2d\varepsilon_{xy} \end{Bmatrix} \tag{8}$$

in which

$$\frac{1}{\omega} = 2(1-\nu)J_2^\sigma - (1-2\nu)\sigma'^2_{zz} - 2(1+\nu)\rho\sigma'_{zz} + 2(1+\nu)\rho^2 + (1-\frac{\alpha I_1^\sigma}{3})\frac{H(1-\nu^2)}{E_o}\sqrt{2J_2^\sigma + 2\rho^2} \tag{9}$$

where E_o is the initial modulus of elasticity, and ν is Poisson's ratio. Further we have that σ'_{xx}, σ'_{yy}, σ'_{zz} are the deviatoric stress components, I_1^σ is the first invariant of the total stresses and J_2^σ is the second invariant of the deviatoric stresses. ρ is given by :

$$\rho = \frac{(\pm 3 - \kappa^2)}{18} I_1^\sigma + \frac{(\beta + \alpha\tau^2)}{3} \tag{10}$$

Φ_{11}, Φ_{12}, Φ_{13}, Φ_{22}, Φ_{23} and Φ_{33} [3,4,5] are functions of Poisson's ratio, the deviatoric stress components and ρ.

The strain-rate function, H, depends upon the current state of stress, strain and straining history. H may be written as :

$$H = (\frac{2}{3})^{1.5} |\bar{\sigma}_{xx}| \frac{E_o E_t}{(E_o - E_t)} \tag{11}$$

where $\bar{\sigma}_{xx}$ is the one-dimensional compressive stress corresponding to the total equivalent plastic strain, which is given by :

$$\bar{\varepsilon}_p = \int d\bar{\varepsilon}^p = \int \sqrt{\frac{2}{3} d\varepsilon_{ij}^p d\varepsilon_{ij}^p} \tag{12}$$

Since $\bar{\varepsilon}^p$ and $\bar{\sigma}_{xx}$ always are related to the compression part of the one-dimensional stress-strain curve, the tangent stiffness, E_t, will also always be from the compression branch of the one-dimensional stress-strain curve.

4. TENSION CRACKING AND CRUSHING OF CONCRETE

If the stress point is outside the failure surface in the tension-compression zone or in the tension-tension zone in Fig. 2a a crack is formed in the plane of the shell element and normal to the greatest principal stress. The direction of this crack will be stored and unaltered through the further calculations. And this crack will influence the local stiffness matrix as long as the strain normal to the crack is greater than zero. If later the second principal stress becomes greater than f_t' an additional crack is formed. The direction of the second crack is not necessary normal to the first crack. Also the second crack direction will be stored and unaltered through the further calculations. The second crack will only influence the local stiffness matrix as long as the strain normal to the crack is greater than zero. Alternatively cracks can also be formed if the strain criterion (14) is exceeded.

When cracking the constitutive matrix is taken to be modified from the initial linear elastic matrix. The total- and incremental-stress normal to the crack drops to zero. If two cracks are formed both normal stresses drop to zero and the stiffness matrix will be a zero matrix except for the diagonal value for eventually retained shear.

The strain criterion of Chen and Chen [3,4,5], which is illustrated in Fig. 2b, is mathematically expressed as :

$$f'(\varepsilon_{ij}) = J_2^{\varepsilon} + \frac{A_u}{3}\frac{\varepsilon_c'}{f_c'} I_1^{\varepsilon} = \tau_u^2 \left(\frac{\varepsilon_c'}{f_c'}\right)^2 \tag{13}$$

or

$$\varepsilon_1 = \varepsilon_t' - \frac{\nu\sigma_2}{E_s} \quad , \varepsilon_2 = \varepsilon_t' - \frac{\nu\sigma_1}{E_s} \tag{14}$$

where I_1^{ε} is the first invariant of the total strains, and J_2^{ε} is the second invariant of the deviatoric strains. ε_1 and ε_2 are the two principle strains, while σ_1 and σ_2 are the stresses in the direction of the principle strains. E_s is the one-dimensional secant stiffness for the stresses σ_1 and σ_2.

If the stresses lies outside the compression-compression failure surface, then the concrete is crushed at this integration point. All stresses then remain at the ultimate level, while the stiffness matrix for the same integration point drops to a zero matrix.

5. THE REINFORCEMENT

The reinforcement is modelled with shell elements placed eccentric to the midpoint of the concrete. The total expressions for the internal forces and the global stiffness matrix are found by summation of the contributions from the elements representing the concrete and the elements representing the reinforcement.

Fig. 3 shows the modelling of the reinforcement bars. θ_1 and θ_2 are the angles between the x-axis and the reinforcement types 1 and 2, respectively. The reinforcement types 1 and 2 have only material stiffness in the directions θ_1 and θ_2, respectively, and a transformation to the x-y system has to be carried out [7].

The reinforcement bars are "smeared out" as a continuous plate, see Fig. 4. The thickness of the equivalent reinforcement layer i is [7]

$$t_i = \frac{n\ A_{si}}{d} \tag{15}$$

in which A_{si} is the cross-sectional area of one bar in the reinforcement layer i, d is the width between the bars and n is the number of reinforcement layers with exactly same material

properties and direction. The concrete is, over the height, "cutted" into a specified number of layers with equal thickness. The numerical integration over the concrete thickness will be by a summation of the influence from each layer.

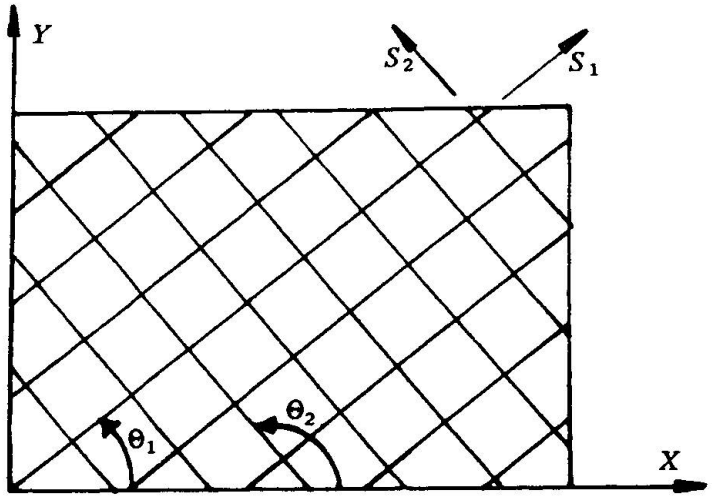

Fig. 3 Reinforcement bars implemented in a membrane element.

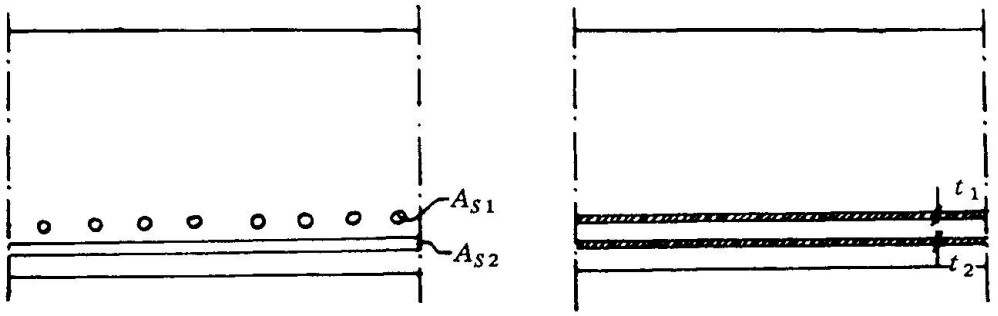

Fig. 4 Idealization of the reinforcement bars.

6. NUMERICAL EXAMPLE

The cylindrical shell roof supported on end diaphragms suggested by Scordelis and Lo [8], has become a classical problem for testing shell elements. The geometry of the shell is given in Fig. 5. For the analysis presented here [9] a 8x8 mesh is used for the nearest quarter of the roof. The accuracy of the 8x8 mesh, and the verification of the shell elements with linear material is well documented in the refs. [1,2], and it is not discussed here.

Fig. 6a shows the material properties for the concrete of quality C45. The compression strains/stresses is according to the norwegian code [10]. The tension strains/stresses are one tenth of the compression strains/stresses. Poisson's ratio is set equal to 0.18. The quality K40TS of the reinforcement is idealized as three straight lines, which is shown in Fig. 6b.

The load-deflection curve of the midpoint of the roof is shown in Fig. 7. The reinforcement was modelled both in $0^o/90^o$ and $45^o/135^o$ to the x-axis. As shown in Fig. 7 the two analysis had the same behaviour up to $P=12.0 \cdot 10^5$N. For higher loads the $0^o/90^o$ analysis was a little bit stiffer. The investigations show further the fault by modelling reinforced concrete structures as a structure with linear behaviour. The first non-linear stadium is a consequence of the non-linearities in the compression part of the equivalent stress/strain curve of Fig. 6a. For concrete

with high f_c/f'_c-ratio the linear behaviour in Fig. 7 would have been higher too.

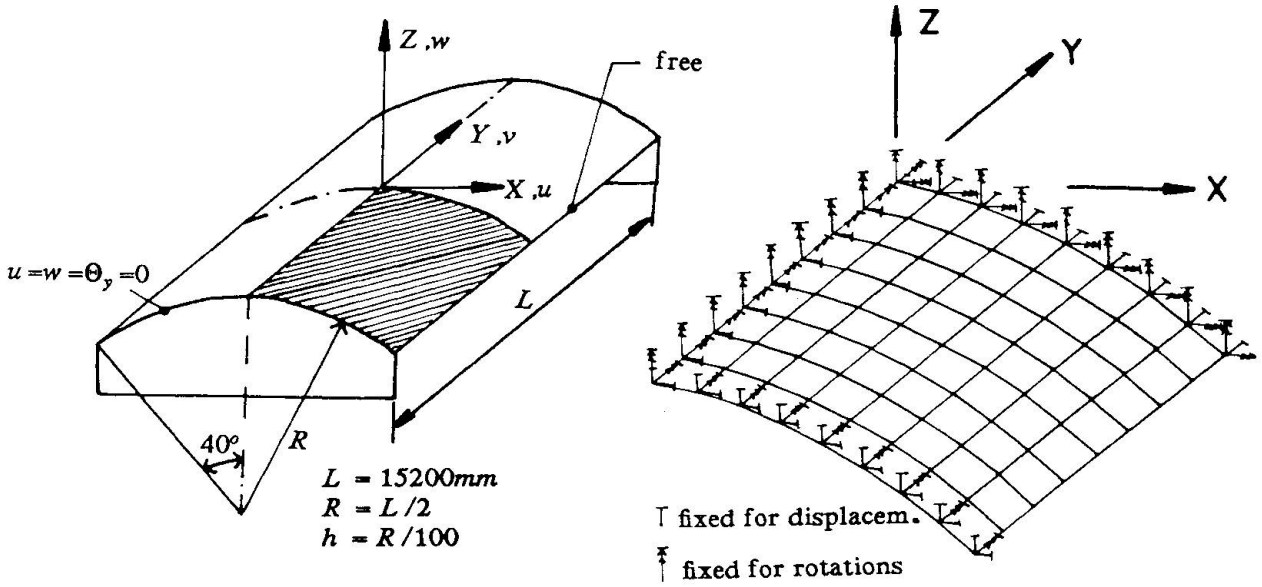

Fig. 5 Cylindrical shell roof

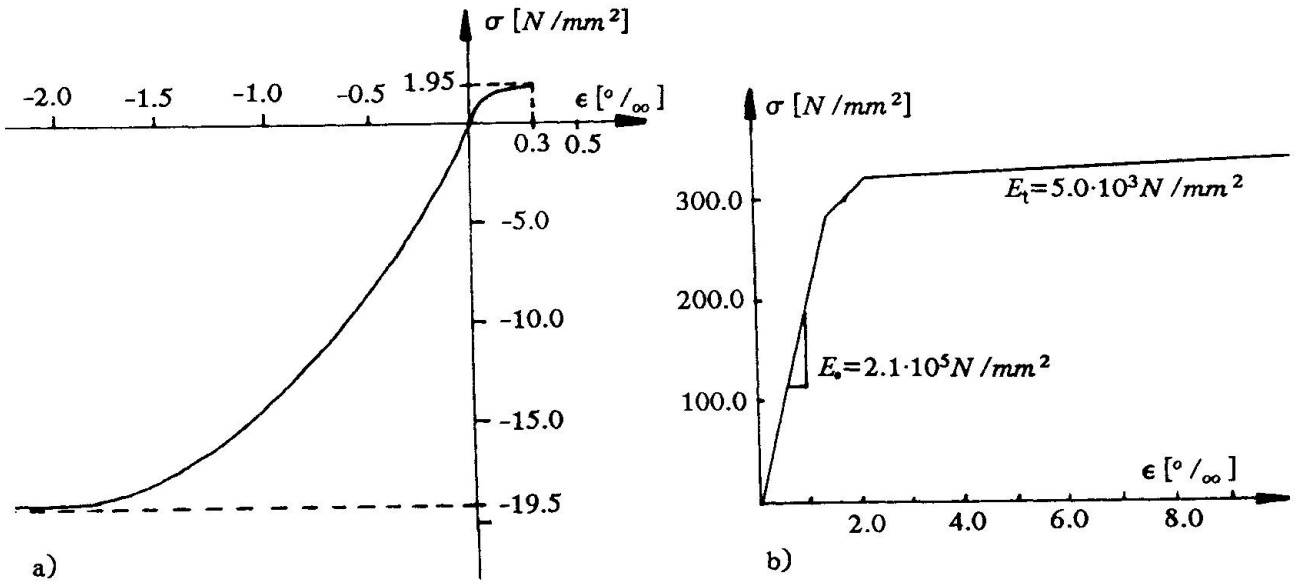

Fig. 6 Equivalent stress/strain relation for a) concrete b) reinforcement

The Fig. 8a show the crack pattern for the integration points in the layer nearest the inside of the roof for three different loads for the $0^o/90^o$ analysis, while the Fig. 8b show the crack pattern for the same integration points for the $45^o/135^o$ analysis for the same three loads. Both analysis show cracking around the load, and cracking around the midpoint of the free side of the roof. This last cracking area was a result of the motion in the x-direction of the elements along the free side of the roof. For this area the shear stresses gave cracking, while under the external load the cracking was a result of bending tensile stresses. The crack propagation in the $0^o/90^o$ analysis has been a little bit less than for the $45^o/135^o$ analysis. And this show clearly that the difference in the crack area is the reason for the difference in the load-deflection at the midpoint in Fig. 7.

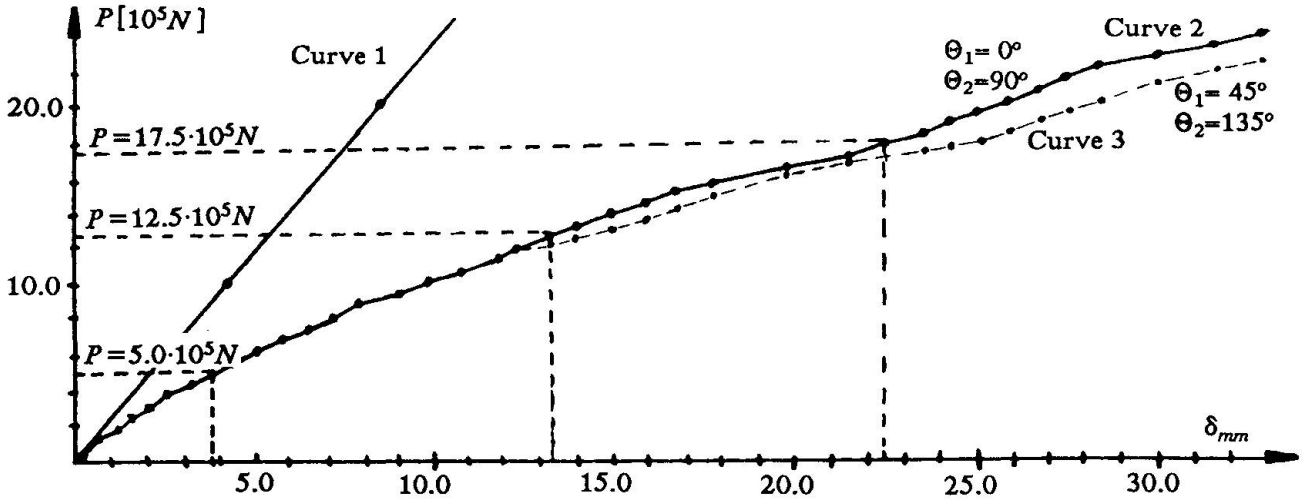

Fig. 7 The load-deflection curve of the midpoint of the roof.

Investigations of the deflection of the roof along the x-axis for $P=5.0\cdot10^5$N showed that the tangent of the deflection curve was horisontal at node 1, while for $P=17.5\cdot10^5$N the deflection curve along the x-axis has no definit tangent at node 1. For this last load the material at node 1 is crushed and cracked, and the stiffness around node 1 is only represented by the reinforcement.

7. CONCLUSIONS

Except for A.C.T.Chen and W.F.Chen's investigations not much experience has previously been gained with their flow theory for large structures. However, the present study shows that the theory is well suited for numerical implementation in shell elements. The greatest weakness of the theory is the assumptions concerning to the coupling between the equivalent stress-strain in tension and compression. Though the strain criteria, in which straining in the opposite direction as loaded is included, does the modell well suited for modelling concrete.

The numerical example demonstrate the applicability and accuracy of the present approaches. The important factors for failure are in many cases cracking and crushing of concrete, yielding of reinforcement, geometric nonlinearities and the size of the load. The accuracy of the results obtained indicates that these factors are well represented in the present approach.

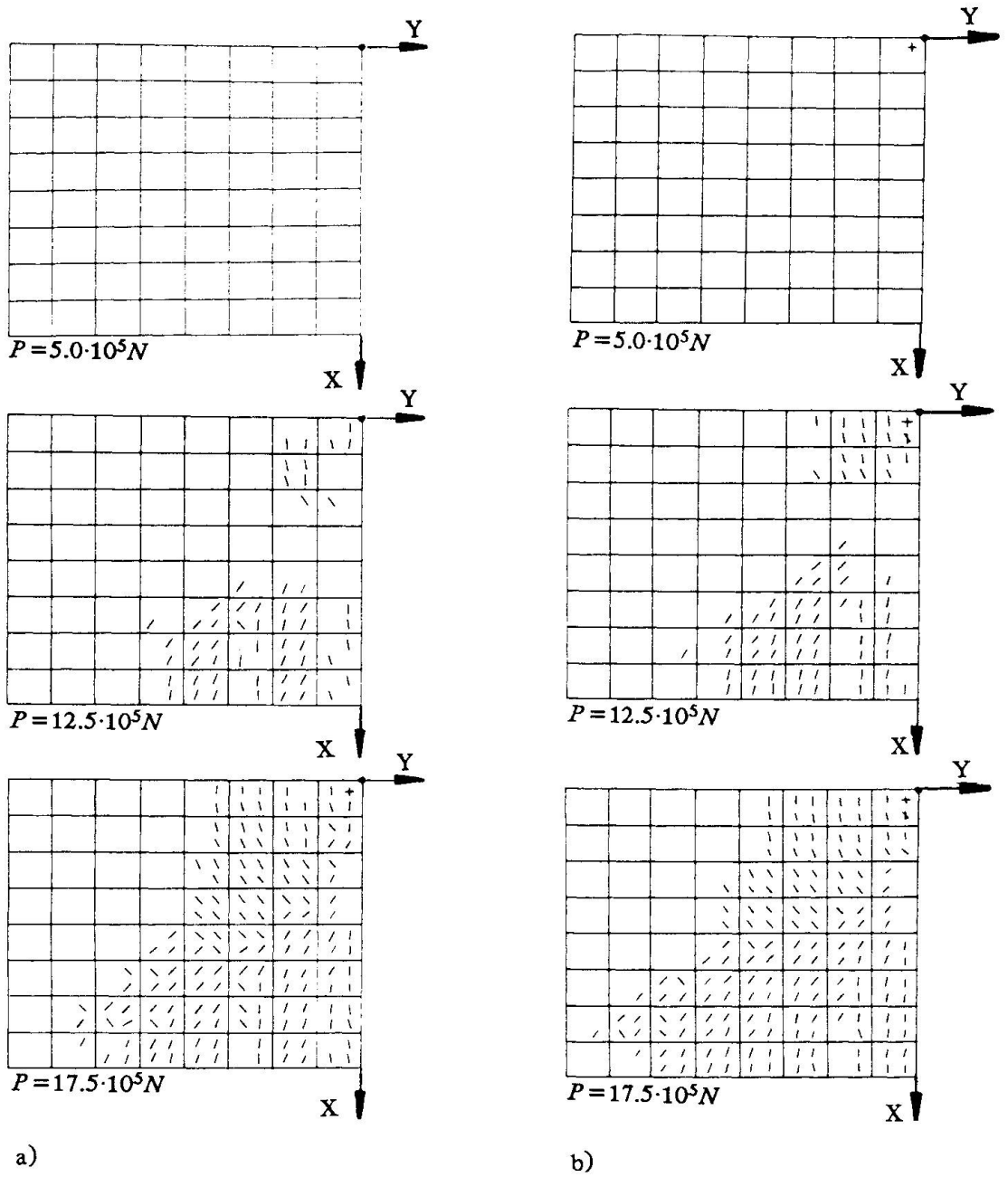

Fig. 8 The crack pattern for a) the $0^o/90^o$ analysis b) the $45^o/135^o$ analysis

7. REFERENCES

1. NYGÅRD, M.K.: "The Free Formulation for Nonlinear Finite Elements with Applications to Shells", Doctoral Thesis, Report no. 86-2, Div. of Struct. Mech., Norwegian Institute of Technology, Norway 1986
2. BERGAN, P.G. and NYGÅRD, M.K.: "Nonlinear Shell Analysis Using Free Formulation Finite Elements", Europe - US Symposium : Finite Element Methods for Nonlinear Problems, Vol. 2, Norway 1985

3. CHEN, A.C.T. and CHEN, W.F.: "Constitutive Relations For Concrete", Journal of the Engineering Mechanics Division, Vol. 101, 1975
4. CHEN, A.C.T. and CHEN, W.F.: "Constitutive Equations and Punch-Indentation of Concrete", Journal of the Engineering Mechanics Division, Vol. 101, 1975
5. CHEN, W.F.: "Plasticity in Reinforced Concrete", McGraw-Hill Book Company, U.S.A. 1982
6. BERGAN, P.G.: "FENRIS-System, Theory-Program Outline-Data Input", NTH-SINTEF-VERITEC, Norway 1986
7. STRØM, O.: "Nonlinear Analysis of Reinforced Concrete Structures Using Beam and Membrane Elements", Doctoral Thesis, Report no. 86-1, Div. of Struct. Mech., Norwegian Institute of Technology, Norway 1986
8. SCORDELIS, A.C. and LO, K.S.: "Computer Analysis of Cylindrical Shells", Journ. of American Concrete Institute, Vol. 61, pp 539-561, 1969
9. VASBOTTEN, A.: "Shell-Elements for Reinforced Concrete", Diploma work, Div. of Struct. Mech., Norwegian Institute of Technology, Norway 1986
10. The norwegian code NS3473 : "Prosjektering av betongkonstruksjoner. Beregning og dimensjonering", NBR, Norway 1982